

CHEMISTRY OF MATERIALS

VOLUME 21, NUMBER 4

FEBRUARY 24, 2009

© Copyright 2009 by the American Chemical Society

Communications

Step-Wise Synthesis of InP/ZnS Core–Shell Quantum Dots and the Role of Zinc Acetate

Euidock Ryu,[†] Sungwoo Kim,[†] Eunjo Jang,[‡] Shinae Jun,[‡] Hyosook Jang,[‡] Byungki Kim,[‡] and Sang-Wook Kim^{*,†}

Department of Molecular Science and Technology, Ajou University, Suwon 443-749, Korea, and Materials & Devices Laboratory, Samsung Advanced Institute of Technology, Samsung Electronics Corp., 449-712 Korea

Received November 12, 2008

Revised Manuscript Received January 8, 2009

Considerable research has been carried out on colloidal semiconductor nanocrystals (NCs) on account of their size dependent electronic and optical properties, which are the key issues in many applications, such as biomedical fluorophores,¹ LEDs,² and photovoltaic devices.³ Among them, a group of II–VI semiconducting NCs, for example, CdSe quantum dots (QDs), exhibit excellent photostability, quan-

tum yield (QY), and a tunable emission wavelength.^{4,16} However, CdSe QDs have limited applications owing to their intrinsic toxicity.⁵ It is believed that III–V QDs, particularly InP NCs, are the most desirable alternative. However, the photoluminescent quantum yield tends to be very low due to nonradiative surface recombination sites and high activation barriers for carrier detrapping.^{6,7} A core–shell structure appears to be essential for surface passivation, but limited numbers have been reported, including InP/ZnS^{8,9,14,15} and InP/ZnCdSe¹⁰ core/shell QDs. HF etching^{11,13} and low reaction temperature methods have also been attempted. In particular, the recent reports by Peng's group on highly luminescent InP/ZnS core–shell quantum dots in the visible range using fatty amine⁹ and Reiss on the one-pot synthesis of InP/ZnS¹⁴ are quite impressive.

We report the stepwise synthesis of InP/ZnS core–shell quantum dots and the role of zinc acetate during the reaction. Zinc acetate was used as a precursor for zinc and acetic acid. Highly luminescent InP/Zn-palmitate was obtained as an intermediate. The InP core was synthesized with indium acetate (In(OAc)₃), tris(trimethylsilyl)phosphine ((TMS)₃P), and palmitic acid as the indium and phosphorus precursors

[†] Ajou University.

[‡] Samsung Electronics Corp.

- (1) (a) Bruchez, M., Jr.; Moronne, M.; Gin, P.; Weiss, S.; Alivisatos, A. P. *Science* **1998**, *281*, 2013–2016. (b) Chan, W. C. W.; Nie, S. *Science* **1998**, *281*, 2016–2018. (c) Medintz, I. L.; Uyeda, H. T.; Goldman, E. R.; Mattoussi, H. *Nat. Mater.* **2005**, *4*, 435–446. (d) Kim, S.; Lim, Y. T.; Soltesz, E. G.; De Grand, A. M.; Lee, J.; Nakayama, A.; Parker, J. A.; Mihaljevic, T.; Laurence, R. G.; Dor, D. M.; Cohn, L. H.; Bawendi, M. G.; Frangioni, J. V. *Nat. Biotechnol.* **2004**, *22*, 93–97. (2) (a) Colvin, V. L.; Schlamp, M. C.; Alivisatos, A. P. *Nature* **1994**, *370*, 354–357. (b) Coe, S.; Woo, W.; Bawendi, M. G.; Bulovic, V. *Nature* **2002**, *420*, 800–803. (c) Tessler, N.; Medvedev, V.; Kazes, M.; Kan, S.; Banin, U. *Science* **2002**, *295*, 1506–1508. (3) (a) Huynh, W. U.; Dittmer, J. J.; Alivisatos, A. P. *Science* **2002**, *295*, 2425–2427. (b) McDonald, S. A.; Konstantatos, G.; Zhang, S. G.; Cyr, P. W.; Klem, E. J. D.; Levina, L.; Sargent, E. H. *Nat. Mater.* **2005**, *4*, 138–142.

- (4) (a) Hines, M. A.; Guyot-Sionnest, P. *J. Phys. Chem.* **1996**, *100*, 468–471. (b) Peng, X.; Schlamp, M. C.; Kadavanich, A. V.; Alivisatos, A. P. *J. Am. Chem. Soc.* **1997**, *119*, 7019–7029. (c) Talapin, D. V.; Rogach, A. L.; Kornowski, A.; Haase, M.; Weller, H. *Nano Lett.* **2001**, *1*, 207–211. (5) (a) Chen, F. Q.; Gerion, D. *Nano Lett.* **2004**, *4*, 1827–1832. (b) Kirchner, C.; Liedl, T.; Kudera, S.; Pellegrino, T.; Javier, A. M.; Gaub, H. E.; Stolzle, S.; Fertig, N.; Parak, W. J. *Nano Lett.* **2005**, *5*, 331–338. (c) Yamazaki, K.; Tanaka, A.; Hirata, M.; Omura, M.; Makita, Y.; Inoue, N.; Sugio, K.; Sigimachi, K. *J. Occup. Health* **2000**, *42*, 169–178. (d) Hardman, R. *Environ. Health Perspect.* **2006**, *114*, 165–172.

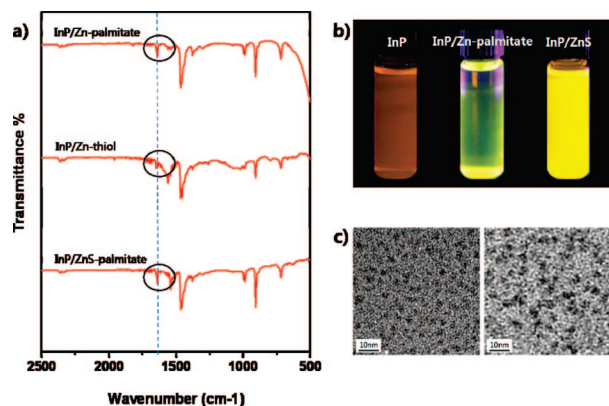


Figure 1. Infrared spectroscopy data (a) and photograph (b) of InP, InP/Zn, and InP/ZnS NCs under UV. TEM images of InP cores (c, left) and InP/ZnS core-shell (c, right).

and stabilizers, respectively, using the methodology reported in Peng and Battaglia's paper.¹² The InP cores had a diameter of ~ 3 nm (Figure 1c, left) and an emission peak in the range of 500–580 nm. Emission peak tuning was made possible by controlling the concentration of the precursors. For example, an emission peak of 580 nm was obtained using 0.06 mmol of indium acetate and 0.03 mmol of (TMS)₃P in 5 mL of octadecene. Another emission peak of 500 nm was achieved at half the concentration in the same volume of solvent. The detailed experimental procedures can be found in the Supporting Information. To achieve the core-shell structure, zinc acetate powder was added to a core solution at ambient temperature under a nitrogen atmosphere. The temperature was then increased to 230 °C and maintained for 5 h. The solution became clear around 100 °C, which means the occurrence of zinc-palmitate and the intensity of photoluminescence started to increase around 150 °C. Figure 1b shows the photographs of the InP cores (left) and InP/Zn-palmitate (center) solutions after cooling. InP/Zn-palmitate was precipitated in octadecene at room temperature (Figure 1b, center), which means palmitic acid cannot play a useful role as a stabilizer any more. The addition of

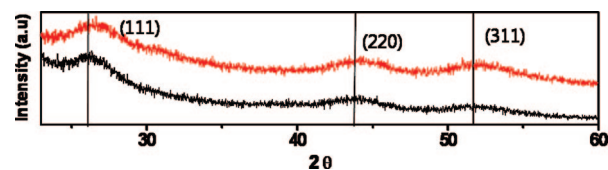


Figure 2. Powder X-ray diffraction of the InP and InP/ZnS core-shell.

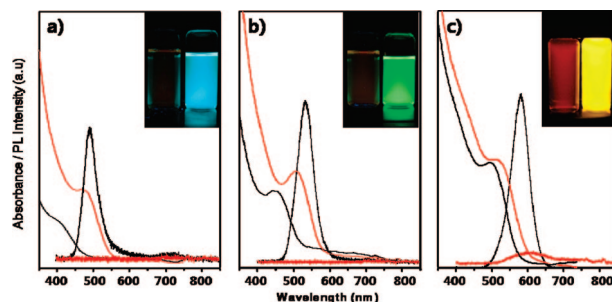


Figure 3. Photoluminescence and absorbance of InP cores (red) and InP/ZnS core shells (black) at each wavelength. Insets show the photograph of InP (left) and InP/ZnS (right) under UV, respectively.

different surfactants, such as dodecanethiol, oleylamine, and trioctylphosphine, made the solution dispersible again. Infrared spectroscopy showed the exchange of surfactants clearly. The carbonyl stretching ($\text{C}=\text{O}$) peaks of palmitate (1640 cm^{-1}) were observed in InP/Zn-palmitate (Figure 1a, top), disappeared in InP/Zn-thiol (Figure 1a, center), and reappeared in InP/ZnS core-shell NCs (Figure 1a, bottom). Disappearance of the carbonyl peak in thiol surfactants means the formation of the InP NCs/Zn–dodecanethiol complex. The bonds between InP NCs and Zn^{2+} ions are quite strong and could survive after surfactant exchange. Existence of zinc was confirmed by inductively coupled plasma atomic emission spectroscopy (ICP-AES) after surfactant exchange. Similarly, the Zn/In ratio was approximately 1.6–1.8 in dodecanethiol, oleylamine, and trioctylphosphine surfactant solution (Zn/In ratio: 1.81 in dodecanethiol, 1.78 in oleylamine, and 1.61 in TOP surfactants solution) when a 2.5 equiv of zinc acetate was used. InP/Zn–dodecanethiol solutions were heated at 230 °C, which resulted in InP/ZnS core-shell quantum dots. The use of alkane thiols as a sulfur precursor in ZnS quantum dots has been reported elsewhere.^{14,16} Similar experiments were performed by the Reiss group.¹⁷ They used zinc stearate and could observe the PL increase, which is explained by the surface passivation of a phosphorus dangling bond by zinc carboxylate. We also conducted similar experiments using zinc palmitate; however, the results are not very impressive compared with zinc acetate. This means that acetate plays an important role in PL increase. The details will be explained in the next page. Powder X-ray diffraction (XRD) showed that the zinc blend structure of the InP and InP/ZnS QDs (Figure 2) were evident, which were indexed to the (111), (220), and (311) planes. The slight shift of peaks between InP and InP/ZnS QDs can demonstrate the existence of ZnS shell structures.¹⁴

Figure 3 shows the photoluminescence and photographs of the InP cores and InP/ZnS core-shells solutions at each wavelength. The core-shell structure led to an improved

- (6) (a) Micic, O. I.; Curtis, C. J.; Jones, K. M.; Sprague, J. R.; Nozik, A. J. *J. Phys. Chem.* **1994**, *98*, 4966–4969. (b) Guzeliyan, A. A.; Katari, J. E. B.; Kadavanich, A. V.; Banin, U.; Hamad, K.; Juban, E.; Alivisatos, A. P.; Wolters, R. H.; Arnold, C. C.; Heath, J. R. *J. Phys. Chem.* **1996**, *100*, 7212–7219. (c) Talapin, D. V.; Rogach, A. L.; Mekis, I.; Haubold, S.; Kornowski, A.; Haase, M.; Weller, H. *Colloids Surf., A* **2002**, *202*, 145–154. (d) Lucey, D. W.; MacRae, D. J.; Furis, M.; Sahoo, Y.; Cartwright, A. N.; Prasad, P. N. *Chem. Mater.* **2005**, *17*, 3754–3762. (e) Xu, S.; Kumar, S.; Nann, T. *J. Am. Chem. Soc.* **2006**, *128*, 1054–1055.
- (7) Kim, S.-H.; Wolters, R. H.; Heath, J. R. *J. Chem. Phys.* **1996**, *105*, 7957–7963.
- (8) Haubold, S.; Haase, M.; Kornowski, A.; Weller, H. *ChemPhysChem* **2001**, *2*, 331–334.
- (9) Xie, R.; Battaglia, D.; Peng, X. G. *J. Am. Chem. Soc.* **2007**, *129*, 15432–15433.
- (10) Micic, O. I.; Smith, B. B.; Nozik, A. J. *J. Phys. Chem. B* **2000**, *104*, 12149–12156.
- (11) Adam, S.; Talapin, D. V.; Borchert, H.; Lobo, A.; McGinley, C.; de Castro, A. R. B.; Haase, M.; Weller, H.; Moller, T. *J. Chem. Phys.* **2005**, *123*, 080706.
- (12) Battaglia, D.; Peng, X. *Nano Lett.* **2002**, *2*, 1027–1030.
- (13) Liu, Z. P.; Kumbhar, A.; Xu, D.; Zhang, J.; Sun, Z. Y.; Fang, J. Y. *Angew. Chem., Int. Ed.* **2008**, *47*, 3540–3542.
- (14) Li, L.; Reiss, P. *J. Am. Chem. Soc.* **2008**, *130*, 11588–11589.
- (15) Xu, S.; Ziegler, J.; Nann, T. *J. Mater. Chem.* **2008**, *18*, 2653–2656.
- (16) Lee, J.; Jun, S.; Jang, E.; Baik, H.; Kim, H.; Cho, J. *Adv. Mater.* **2007**, *19*, 1927–1932.

- (17) Li, L.; Protiere, M.; Reiss, P. *Chem. Mater.* **2008**, *20*, 2621–2623.

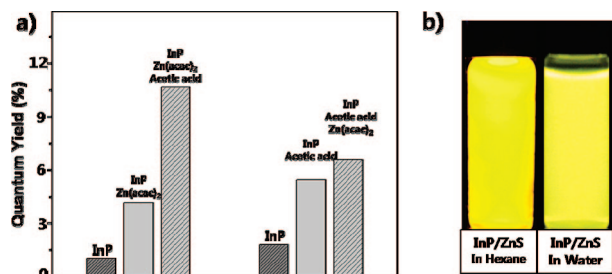


Figure 4. Comparison data of PL intensities under the same absorption at 400 nm; InP core \rightarrow Zn(acac)₂ added \rightarrow acetic acid added (a, left), InP core \rightarrow acetic acid added \rightarrow Zn(acac)₂ added (a, right). Photographs of InP/ZnS NCs in hexane (b, left) and water (b, right).

quantum yield of 38% (Figure 3c), 18% (Figure 3b), and 7% (Figure 3a), and a blue-shift in absorption and emission. The blue-shift was larger in the NCs with short-wavelength absorption than in those absorbing in a longer-wavelength. (Figure 3: part a, 72 nm; part b, 53 nm; and part c, 24 nm) A lower or higher reaction temperature also improved the quantum yield, but the effects were not as impressive as that at 230 °C. The blue-shift in absorption and emission was attributed to etching by acetic acid, which originated from zinc acetate, and was similar to HF etching.¹¹ Hence, acetic acid, which is the reaction product of zinc acetate and palmitic acid, etched the surface of the core leading to the easy formation of the shell. This hypothesis can explain the large blue-shift in smaller NCs (Figure 3a: short-wavelength absorption). The following experiments were carried out to test the hypothesis. A slight increase in quantum yield was obtained using zinc acetylacetonate (Zn(acac)₂) as a zinc precursor instead of zinc acetate. Acetic acid was added continuously resulting in a more than two-fold increase in quantum yield. The reverse stepwise addition of acetic acid and Zn(acac)₂ showed a similar tendency, but the effects were not as pronounced. Detailed comparison data can be found in Figure 4. After all, zinc acetate plays an important role in surface etching and ZnS shell formation, which results in a blue-shift in emission (or absorption) and an improvement in quantum yield. To study the quantitative effect, the amounts of zinc acetate were controlled from 1 equiv to 5 equiv based on phosphorus. Figure 5 shows that Zn to P precursor ratios of 1/1, 3/1, and 5/1 result in a blue-shift in the absorption peak of 9 nm, 15 nm, and 22 nm, respectively. The quantum yield of the core-shell was 8%, 20%, and 38% at a Zn:P ratio of 1, 3, and 5, respectively. Above 5 equiv, the quantum yield began to decrease. X-ray photoelectron spectroscopy (XPS) (Figure S2, Supporting Information) and ICP-AES demonstrated the existence of zinc. ICP-AES of

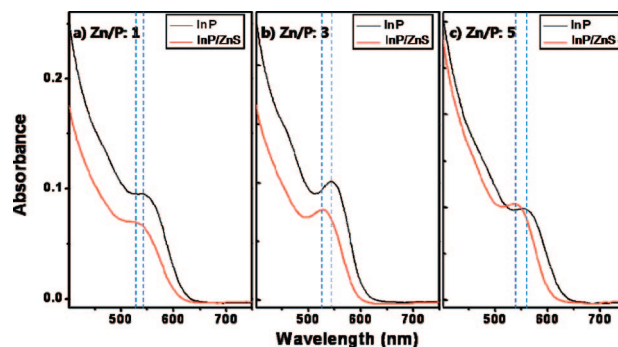


Figure 5. Absorbance of InP cores (black) and InP/ZnS core/shells (red) at each amount of Zn.

the subsequent sample (Zn/P = 1, 3, and 5) showed an increasing tendency, a zinc to phosphorus ratio of 0.54, 1.48, and 1.99, respectively.

Transmission electron microscopy (TEM) revealed InP cores and InP/ZnS core-shells, 2.9 nm ($\sigma = 0.19$) and 3.5 nm ($\sigma = 0.23$) in diameter, respectively (Figure 1c). The wide low resolution and magnified images are shown in Supporting Information. The quantum dots were transferred to water to check the stability of the ZnS shell, and highly luminescent water-dispersible quantum dots were obtained (Figure 4b).

The stability tests of the InP/ZnS core-shell nanocrystals using both the conventional method⁸ and the procedure reported in this paper were conducted under ambient (room temperature and light) and heat-aged (dark and 120 °C for 12 h) conditions. Both data showed the superior properties of InP/ZnS core-shell NCs by our method (Supporting Information).

In conclusion, highly luminescent and stable InP/ZnS core-shell nanocrystals were developed by stepwise addition of zinc acetate and dodecanethiol to an InP core solution. Zinc acetate plays an important role in surface etching and ZnS shell formation.

Acknowledgment. This work was supported by Samsung Electronics and Grant R01-2006-000-10271-0 from the Basic Research Program of the Korea Science & Engineering Foundation and a grant from the Fundamental R&D program for Core Technology of Materials funded by the ministry of Commerce, Industry and Energy.

Supporting Information Available: Detailed experimental procedures, XPS data of InP and InP/ZnS NCs, and stability data of InP/ZnS core-shell NCs (PDF). This material is available free of charge via the Internet at <http://pubs.acs.org>.

CM803084P